Journal of Veterinary Science

JVS

Original Article
Pharmacology

Check for updates

Antibacterial activity of enrofloxacin loaded gelatin-sodium alginate composite nanogels against intracellular *Staphylococcus aureus* small colony variants

Wanhe Luo [1,2], Jinhuan Liu [1], Samah Attia Algharib [3], Wei Chen [1,2,*]

[1]Engineering Laboratory for Tarim Animal Diseases Diagnosis and Control, College of Animal Science, Tarim University, Alar 843300, China
[2]Key Laboratory of Tarim Animal Husbandry & Science Technology of Xinjiang Production & Construction Corps, Alar 843300, China
[3]Department of Clinical Pathology, Faculty of Veterinary Medicine, Benha University, Moshtohor, Toukh 13736, Egypt

🔓 OPEN ACCESS

*Corresponding author:
Wei Chen
Engineering Laboratory for Tarim Animal Diseases Diagnosis and Control, College of Animal Science, Tarim University; Key Laboratory of Tarim Animal Husbandry & Science Technology of Xinjiang Production & Construction Corps., Alar, Xinjiang 843300, China.
Email: 379497687@qq.com
https://orcid.org/0000-0003-2336-0108

ABSTRACT

Background: The poor intracellular concentration of enrofloxacin might lead to treatment failure of cow mastitis caused by *Staphylococcus aureus* small colony variants (SASCVs).
Objectives: In this study, enrofloxacin composite nanogels were developed to increase the intracellular therapeutic drug concentrations and enhance the efficacy of enrofloxacin against cow mastitis caused by intracellular SASCVs.
Methods: Enrofloxacin composite nanogels were formulated by an electrostatic interaction between gelatin (positive charge) and sodium alginate (SA; negative charge) with the help of $CaCl_2$ (ionic crosslinkers) and optimized by a single factor test using the particle diameter, zeta potential (ZP), polydispersity index (PDI), loading capacity (LC), and encapsulation efficiency (EE) as indexes. The formation mechanism, structural characteristics, bioadhesion ability, cellular uptake, and the antibacterial activity of the enrofloxacin composite nanogels against intracellular SASCVs strain were studied systematically.
Results: The optimized formulation was comprised of 10 mg/mL (gelatin), 5 mg/mL (SA), and 0.25 mg/mL ($CaCl_2$). The size, LC, EE, PDI, and ZP of the optimized enrofloxacin composite nanogels were 323.2 ± 4.3 nm, 15.4% ± 0.2%, 69.6% ± 1.3%, 0.11 ± 0.02, and −34.4 ± 0.8 mV, respectively. Transmission electron microscopy showed that the enrofloxacin composite nanogels were spherical with a smooth surface and good particle size distributions. In addition, the enrofloxacin composite nanogels could enhance the bioadhesion capacity of enrofloxacin for the SASCVs strain by adhesive studies. The minimum inhibitory concentration, minimum bactericidal concentration, minimum biofilm inhibitory concentration, and minimum biofilm eradication concentration were 2, 4, 4, and 8 µg/mL, respectively. The killing rate curve had a concentration-dependent bactericidal effect as increasing drug concentrations induced swifter and more radical killing effects.
Conclusions: This study provides a good tendency for developing enrofloxacin composite nanogels for treating cow mastitis caused by intracellular SASCVs and other intracellular bacterial infections.

Keywords: Enrofloxacin; *Staphylococcus aureus*; Nanogels; sodium alginate; gelatin

Generated by xmlinkpress

ORCID iDs
Wanhe Luo
https://orcid.org/0000-0002-5170-1670
Jinhuan Liu
https://orcid.org/0000-0003-4978-2229
Samah Attia Algharib
https://orcid.org/0000-0002-3336-2855
Wei Chen
https://orcid.org/0000-0003-2336-0108

Author Contributions
Conceptualization: Luo W; Data curation: Luo W, Liu J; Formal analysis: Luo W; Funding acquisition: Luo W; Investigation: Luo W; Methodology: Luo W, Liu J; Project administration: Luo W; Software: Algharib SA; Supervision: Luo W, Chen W; Validation: Chen W; Visualization: Luo W; Writing - original draft: Luo W, Algharib SA; Writing - review & editing: Luo W, Algharib SA, Chen W.

Conflict of Interest
The authors declare no conflicts of interest.

INTRODUCTION

The increasing incidence of facultative or obligate intracellular bacterial infections poses a considerable health threat for humans and animals worldwide [1]. For example, cow mastitis caused by *Staphylococcus aureus* is becoming increasingly serious in the dairy industry [2-4]. In particular, *S. aureus* small colony variants (SASCVs) in host cells could establish reservoirs from which reinfections can occur, resulting in long-term and repeated infections [5]. Enrofloxacin is used intensively to treat various intracellular bacteria (e.g., SASCVs cow mastitis) in the veterinary field because of its strong antibacterial properties [6]. On the other hand, the intracellular concentration of enrofloxacin is relatively weak. It was reported that when the cells were incubated with the free enrofloxacin (10 µg/mL) for 0.25, 0.5, 1, 2, and 4 h, it reached a maximum concentration of only 0.03 µg/mg protein at 0.25 h [7]. Although high-dose drugs can have better curative effects, they will increase the treatment cost, cause side effects, and increase drug residues resistance [8]. Therefore, there is urgent need to develop novel smart delivery systems to increase the intracellular therapeutic drug concentrations, thus enhancing the efficacy of enrofloxacin against cow mastitis caused by the SASCVs strain.

Liu et al. [9] reported an increase in the enrofloxacin concentration in *S. aureus* biofilms by enhancing the bioadhesion ability of antibacterial agents. Thus, the intracellular therapeutic drug concentrations might be increased by modifying the bioadhesive ability of antibacterial agents to bacteria. Nanogels, nanosized hydrogels, have the advantages of both nanoparticles and hydrogels. Nanogels are used to incorporate drugs because they are nanosized crosslinked polymeric networks [10]. Nanogels can act as effective delivery systems to increase intracellular drug concentrations because of their excellent structural stability and bioadhesion performance on bacteria [11]. The bioadhesion capacity is determined by the adhesive materials. Some researchers showed that gel materials hold excellent bioadhesion capacity, e.g., sodium alginate (SA) with a negative charge used as a drug delivery system [12]. Zhou et al. [13] developed tilmicosin-loaded SA-chitosan composite nanogels that could enhance the antibacterial activity of enrofloxacin against *S. aureus* cow mastitis caused by the excellent bioadhesion capacity of SA. In addition, gelatin was reported to be an effective material to prepare nanogels with increasing drug concentration at the bacterial infection site and controlling drug release [14]. For example, curcumin encapsulated pH-sensitive gelatin-based interpenetrating polymeric network nanogels could be conducive to anticancer drug delivery in host cells [15]. Thus, the enrofloxacin composite nanogels may be formulated by electrostatic interactions between gelatin (positive charge) and SA (negative charge) with the help of $CaCl_2$ (ionic crosslinkers). The prepared enrofloxacin-loaded gelatin-SA composite nanogels can enhance the antibacterial activity by improving the bioadhesion capacity of the enrofloxacin for SASCVs strain. This will increase the intracellular therapeutic drug concentrations and prolong the action time between the enrofloxacin composite nanogels and the SASCVs strain, which will be more conducive to killing bacteria [16-18]. More importantly, composite nanogels are safe and more efficacious because they are biocompatible and less degradable and toxic [19]. Thus, enrofloxacin-loaded gelatin-SA composite nanogels are promising as a biocompatible preparation for SASCVs strain.

This study hypothesized that the enrofloxacin-loaded gelatin-SA composite nanogels would enhance the bioadhesion capacity of enrofloxacin to intracellular SASCVs strain, thereby increasing intracellular therapeutic drug concentrations and the antibacterial effect of enrofloxacin against cow mastitis caused by the SASCVs strain (**Fig. 1**).
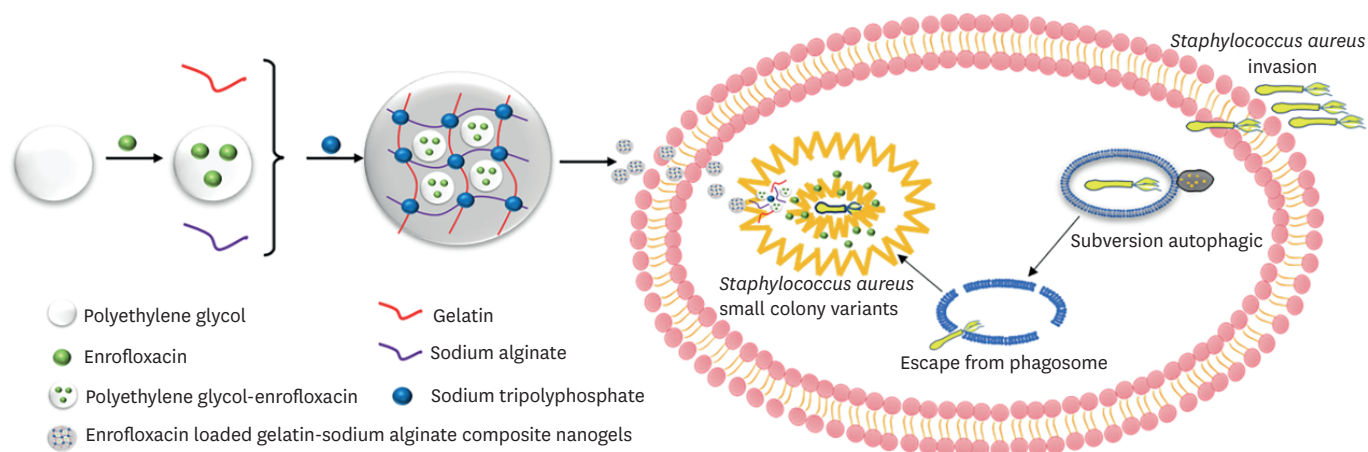
Fig. 1. Schematic diagram describing the synthesis of enrofloxacin-loaded gelatin-sodium alginate composite nanogels.

In this study, the enrofloxacin-loaded gelatin-SA composite nanogels were designed by electrostatic interactions with the help of an ionic crosslinker and optimized by the single factor test using the particle diameter, zeta potential (ZP), polydispersity index (PDI), loading capacity (LC), and encapsulation efficiency (EE) as indices. The formation mechanism, structural characteristics, bioadhesion ability, cellular uptake, and the antibacterial activity of enrofloxacin composite nanogels against intracellular SASCVs strain were studied systematically.

MATERIALS AND METHODS

Materials
Enrofloxacin (≥ 95.5%) and enrofloxacin solution (10%) were bought from Hubei Widely Chemical Technology (China). The enrofloxacin standard (98%) was purchased from the China Institute of Veterinary Drugs Control (China). RAW 264.7 cells were provided by the National Veterinary Drug Residues Reference Laboratory of Huazhong Agricultural University (China). Dulbecco's Modified Eagle Medium was obtained from Hyclone (USA). Bisbenzimide H 33342 trihydrochloride (Hoechst 33342), 1,1′-dioctadecyl-3,3,3′,3′-tetramethylindocarbocyanine perchlorate (DiI), RIPA cell lysate, and the bicinchoninic acid (BCA) test kit were acquired from Xinjiang Tongjin Zhiyang Biotechnology (China). SA (molecular weight (MV): 398.32; viscosity: ≥ 0.02 Pa.s in 10 g/L, 20°C), gelatin (≥ 99%; MV: 5,000), polyethylene glycol (PEG; MV: 697.61), sodium tripolyphosphate (MW: 367.86), and fluorescein isothiocyanate isomer I (FITC, MW: 389.39) were purchased from Tata gene (China). The water was prepared using a Milli-Q system (Millipore, USA). Other chemicals and reagents used in this study were of high analytical grade.

Bacteria
SASCVs were provided by the College of Veterinary Medicine of China Agricultural University.

Formulation of enrofloxacin-loaded gelatin-SA composite nanogels
The enrofloxacin-loaded gelatin-SA composite nanogels were formulated by an electrostatic interaction using an ionic crosslinker according to a previous report with some modifications [9]. Briefly, SA (5, 10, or 15 mg/mL) was added to ultrapure water with magnetic stirring for complete dissolution. Simultaneously, gelatin (10, 20, or 30 mg/mL) was completely

dissolved in ultrapure water at pH 5.5. Subsequently, $CaCl_2$ (0.25, 0.5, or 1 mg/mL) solution added into the gelatin solution by drops. Subsequently, 1 g of enrofloxacin and 2 g of PEG were weighed into a 100 mL beaker containing 10 mL of 0.1 M NaOH. The enrofloxacin solution was added to a gelatin solution at a flow rate of 0.1 mL/min with magnetic stirring. Finally, the gelatin mixture was added dropwise to the SA solution with magnetic stirring at 1,800 rpm to form the enrofloxacin-loaded gelatin-SA composite nanogel. The optimal amounts of SA, gelatin, and $CaCl_2$ were evaluated by an orthogonal experiment using the particle diameter, ZP, PDI, LC, and EE as indices. Each sample was formulated three times. The data are expressed as the mean ± SD. The FITC-labeled enrofloxacin-loaded gelatin-SA composite nanogels were prepared, as described previously [7]. Briefly, the FITC-labeled enrofloxacin-loaded gelatin-SA composite nanogels were formulated by adding 1 mg of FITC into 10 mL enrofloxacin composite nanogels.

Characterization of enrofloxacin composite nanogels

Determination of particle diameter, ZP, and PDI
The particle diameter, ZP, and PDI of the different enrofloxacin-loaded gelatin-SA composite nanogels were determined using a Zeta sizer ZX3600 (Malvern Instruments, USA). Before the measurement, enrofloxacin composite nanogels were properly diluted to obtain the optimal kilo counts per second.

Quantitative measurement of enrofloxacin composite nanogels
A method for determining the enrofloxacin concentration by high-performance liquid chromatography (HPLC) was established, and the specificity, accuracy, linearity, and precision were validated. The chromatographic conditions were as follows: column, Agilent SB C_{18} (250 mm × 4.6 mm × 5 μm); detection wavelength, 278 nm; column temperature, 25℃; mobile phase, 0.1% formic acid (phase A) and acetonitrile (phase B) with a ratio of 86:14; flow rate, 1.00 mL/min; injection volume, 40 μL. The enrofloxacin concentration was determined from a standard curve.

Determination of the LC and EE
The different enrofloxacin composite nanogels samples were obtained by centrifugation at 12,000 RPM for 60 min at 4℃. After centrifugation, the enrofloxacin in the supernatant was tested by HPLC to calculate EE. The precipitation was lyophilized into powder after re-suspending to calculate LC.

Determination of sedimentation rate (F)
The original height (H_0) of 30 mL of the enrofloxacin composite nanogels sample in 100 mL graduated cylinder after shaking was measured. The height (H) of the sediment in the cylinder after standing for 3 h was recorded. F was calculated according to the equation [11]: $F = H/H_0$.

Transmission electron microscopy (TEM)
A 2 μL enrofloxacin composite nanogels sample was added to copper grids with thin slices and dried at room temperature with negative staining by sodium phosphotungstate (2%). The morphology was observed by TEM (TF20, JOEL 2100F).

Internalization and distribution of nanogels in cells

The RAW 264.7 cells ($1 × 10^5$ cells/cm^2) were seeded on a 24-well cell culture plate. After 24 h, the cells were incubated with the same concentration (4 μg/mL) of native enrofloxacin and composite nanogels for 0.5, 1, 2, and 4 h. After washing three times with cold phosphate-

buffered saline (PBS), the adherent cells were lysed using 150 μL of RIPA cell lysate. The protein content and the concentration of enrofloxacin in the cells were detected using the BCA method and HPLC, respectively.

Simultaneously, the RAW 264.7 cells (1×10^5/dish) were transferred to a confocal dish. After incubation for 24 h, the FITC-labeled enrofloxacin nanogels with the same fluorescence intensity were transferred to the RAW 264.7 cells and incubated for 2 h. After washing three times with PBS, the RAW 264.7 cells were then stained with DiI and Hoechst 33342 for membrane and nuclear staining. The cells were visualized by confocal laser scanning microscopy (Zeiss, Germany) to observe the location of the nanogels in the RAW 264.7 cells.

Adhesive studies

The enrofloxacin composite nanogels were placed into the liquid medium containing the SASCVs strain of logarithmic growth phase of 10^6 CFU/mL at the final enrofloxacin concentrations of 4 μg/mL. The liquid culture was drawn on the copper mesh after incubation for 30 min and observed by scanning electron microscopy (SEM, SIGMA HD) to determine if the enrofloxacin composite nanogels had been adsorbed on the surface of bacteria.

Intracellular antibacterial activity

Minimum inhibitory concentration (MIC) and minimum bactericidal concentration (MBC)
After incubation of the 10^7 CFU/mL SASCVs strain with RAW 264.7 cells in 24-well culture plates for 2 h, the extracellular bacteria were removed and incubated with gentamicin at 100 μg/mL for 0.5 h to kill the extracellular SASCVs strain [7]. After washing with 4°C PBS, the RAW 264.7 cells were added with 0.1 mL of the enrofloxacin composite nanogels (128, 64, 32, 16, 8, 4, 2, and 1 μg/mL) in each well, respectively. The positive control (SASCVs strain in RAW 264.7 cells) and negative control (RAW 264.7 cells) were also included. The MIC value was considered the value at the lowest concentration of enrofloxacin composite nanogels that inhibited bacterial density by 99.9%. The MBC value was considered the value at the lowest concentration of enrofloxacin composite nanogels that inhibited the bacterial density by 99.99%.

Minimum biofilm inhibitory concentration (MBIC) and minimum biofilm eradication concentration (MBEC)
The MBIC and MBEC were determined as described elsewhere with some modifications [20]. Briefly, after SASCVs strain biofilms formation in 24-well plates at 37°C for 24 h, the medium was gently removed; the wells were washed with PBS, and serial dilutions of 0.1 mL enrofloxacin composite nanogels (128, 64, 32, 16, 8, 4, 2, and 1 μg/mL) were added. The positive and negative controls represented by enrofloxacin composite nanogels-free wells and biofilm-free wells, respectively, were also included. MBIC was defined as the lowest concentration of enrofloxacin composite nanogels inhibiting the visible growth after 24 h incubation. Wells with no visible growth were washed with PBS; the adherent bacteria were removed mechanically and spread on plates. The MBEC was determined as the lowest concentration at which no growth occurred.

Intracellular killing rate curve
After incubating the 10^7 CFU/mL SASCVs strain with RAW 264.7 cells in 24-well culture plates for 2 h, the extracellular bacteria were removed and incubated with gentamicin at 100 μg/mL for 0.5 h to kill the extracellular SASCVs strain. After washing with 4°C PBS, different concentrations of enrofloxacin composite nanogels (1/2 × MIC, 1 × MIC, 2 × MIC, and 4 × MIC) were added to RAW 264.7 cells in each well. After 0, 1, 2, 4, 8, 12, 24, 48, and 72 h of

incubation, the washed cells were lysed and spread on plates to determine the number of viable SASCVs by colony counting. The time-kill curves were drawn by plotting the average counts as a function of time.

Statistical analysis
The experiment data are expressed as the mean ± SD and analyzed by the one-way analysis of variance using SPSS software (IBM, USA); p values < 0.05 were considered significant.

RESULTS

Optimization of enrofloxacin loaded gelatin-SA composite nanogels
Enrofloxacin composite nanogels were produced by an electrostatic interaction between gelatin (positive charge) and SA (negative charge) using $CaCl_2$ (crosslinkers). The concentrations of SA, gelatin, and $CaCl_2$ were selected as variables. LC, EE, size, ZP, and PDI are important parameters for the preparation of drugs [21]. Thus, the enrofloxacin composite nanogels were optimized by a single factor test using EE, LC, size, ZP, and PDI as the assessment indices. The concentrations of SA, gelatin, and $CaCl_2$ have a great influence on the mean EE, LC, sizes, PDI, and ZP of enrofloxacin composite nanogels (**Table 1**). The optimal composite nanogel was obtained when the particle size and PDI of the enrofloxacin-loaded gelatin-SA composite nanogels were the smallest, and the ZP, EE, and LC were the largest. Thus, the final optimal formula was comprised of 10 mg/mL (gelatin), 5 mg/mL (SA), and 0.25 mg/mL ($CaCl_2$).

Properties of enrofloxacin composite nanogels
Enrofloxacin showed a linear range from 0.05 to 20 µg/mL (r = 0.9993). The limit of detection was 0.04 µg/mL, and the limit of quantification was 0.05 µg/mL. The mean recovery of enrofloxacin was 96.3%–98.9%. The relative SD of enrofloxacin were below 1.2% for the intra-day and inter-day variations. The specificity of the method was good for the target substances without endogenous interference on the chromatograms. The enrofloxacin composite nanogels were a homogenous canary yellow uniform suspension with a sedimentation rate of 1 (**Fig. 2A**). The mean EE, LC, sizes, PDI, and ZP of the optimal enrofloxacin composite were 15.4% ± 0.2%, 69.6% ± 1.3%, 323.2 ± 4.3 nm (**Fig. 2B**), 0.11 ± 0.02, and −34.4 ± 0.8 mv (**Fig. 2C**), respectively. TEM showed that the enrofloxacin composite nanogels were spherical with a smooth surface and good particle size distributions (**Fig. 2D**).

Table 1. Optimization of enrofloxacin-loaded gelatin-SA composite nanogels (mean ± SD, n = 3)

Gelatin (mg/mL)	SA (mg/mL)	$CaCl_2$ (mg/mL)	Size (nm)	ζ Potential (mV)	PDI	EE (%)	LC (%)
30	5	0.25	657.4 ± 3.2	−26.5 ± 1.2	0.13 ± 0.23	8.7 ± 0.3	47.4 ± 1.0
10	10	0.25	785.3 ± 4.1	−26.9 ± 0.5	0.33 ± 0.04	11.2 ± 0.2	52.5 ± 1.8
20	15	0.25	918.1 ± 5.7	−27.3 ± 1.2	0.47 ± 0.15	13.8 ± 0.4	64.3 ± 1.5
20	10	1.00	843.2 ± 3.7	−28.6 ± 1.6	0.59 ± 0.26	13.7 ± 0.5	57.4 ± 2.3
30	10	0.50	807.4 ± 3.3	−29.5 ± 0.7	0.55 ± 0.07	13.2 ± 1.1	60.5 ± 0.5
20	5	0.50	787.3 ± 1.9	−35.0 ± 0.4	0.57 ± 0.22	12.8 ± 1.2	58.3 ± 1.7
10	5	0.25	323.2 ± 1.0	−34.4 ± 1.1	0.11 ± 0.04	15.4 ± 0.3	69.6 ± 0.3
30	15	1.00	1,008.7 ± 2.4	−33.5 ± 1.0	0.62 ± 0.05	14.8 ± 0.1	63.1 ± 0.6
10	5	1.00	408.4 ± 5.3	−31.5 ± 2.8	0.35 ± 0.27	12.7 ± 1.8	65.4 ± 2.8

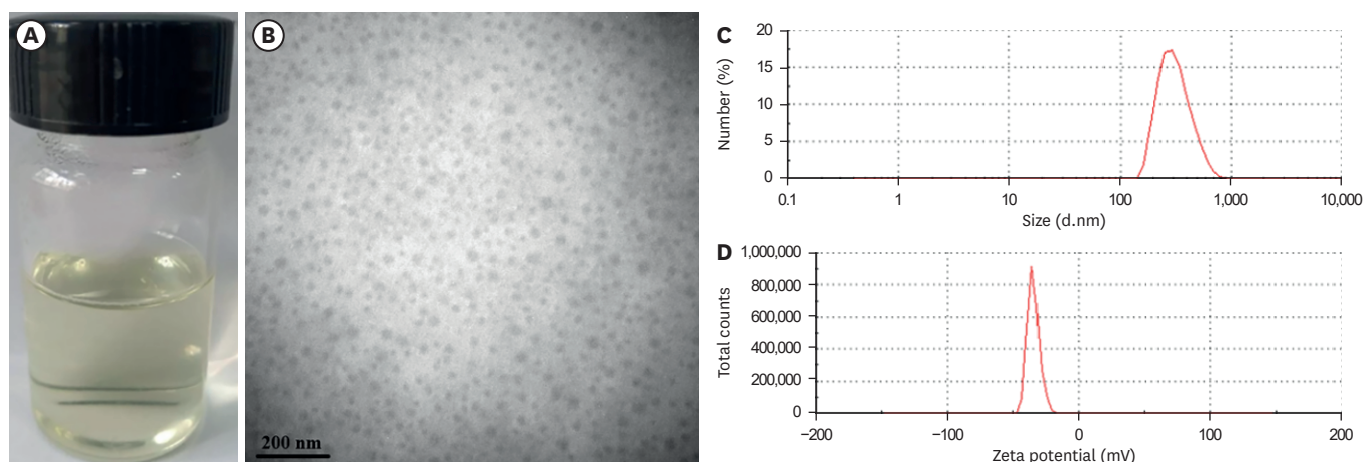SA, sodium alginate; PDI, polydispersity index; EE, encapsulation efficiency; LC, loading capacity.

Fig. 2. Properties of the optimal enrofloxacin composite nanogels. (A) Appearance; (B) Transmission electron microscopy images; (C) Size distribution; (D) Zeta potential.

Internalization and distribution of enrofloxacin composite nanogels in RAW 264.7 cells

The drug uptake in the RAW 264.7 cells was determined by incubating with 4 μg/mL native enrofloxacin and the enrofloxacin composite nanogels for 0.5, 1, 2, and 4 h. The composite nanogels enhanced the intracellular concentrations of enrofloxacin (**Fig. 3**). After 0.5 h of incubation, the intracellular concentrations of native enrofloxacin and enrofloxacin-loaded gelatin-SA composite nanogels were 0.09 ± 0.04, and 0.66 ± 0.04 μg/mg protein, respectively. Subsequently, native enrofloxacin and enrofloxacin-loaded gelatin-SA composite nanogels reached the maximum intracellular concentrations of 0.17 ± 0.08, and 0.89 ± 0.05 μg/mg protein, respectively, within the first 2 h under an incubation concentration of 10 μg/mL. The amount of enrofloxacin composite nanogels accumulated in the macrophages was approximately 5.23 times higher than the native enrofloxacin after 2 h of incubation. These results show that enrofloxacin composite nanogels could enhance intracellular enrofloxacin accumulation more significantly than the native enrofloxacin (**Fig. 3A**). Confocal microscopy also confirmed that a large amount of FITC-labeled nanogel had entered the cells after 2 h of incubation (**Fig. 3B-D**). The labeled green fluorescence of the nanogels is distributed mainly around the perinuclear. The labeled green fluorescence of the enrofloxacin composite nanogels was stronger than the native enrofloxacin. The enrofloxacin composite nanogels were internalized more easily into RAW 264.7 cells than native enrofloxacin.

Adhesive studies

In this study, the co-culture of SASCVs and enrofloxacin composite nanogels for 30 min were observed by SEM. SEM showed that the enrofloxacin composite nanogels were contacted with or absorbed on the SASCVs strains (**Fig. 4A**). Energy dispersive spectrometry images displayed that enrofloxacin composite nanogels could enter SASCVs strain well and have good biocompatibility (**Fig. 4B-E**).

Antibacterial activity

The positive control showed turbidity, indicating that the bacteria were not inhibited. The negative control showed clarity, indicating no bacterial growth. The MIC, MBC, MBIC, and MBEC of the enrofloxacin composite nanogels against SASCVs strain were 2, 4, 4, and 8 μg/mL, respectively. According to the killing rate curve, the enrofloxacin composite nanogels had a concentration-dependent bactericidal effect as increasing drug concentrations induced
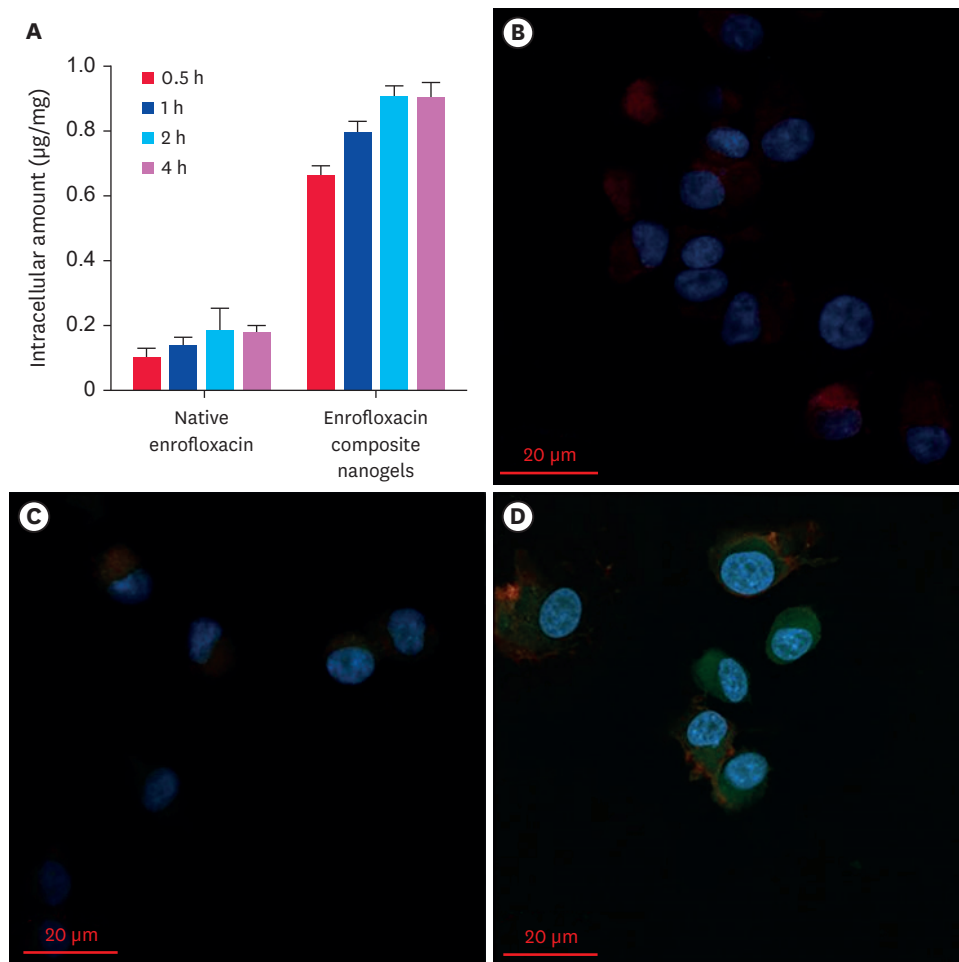
Fig. 3. Uptake of native enrofloxacin and enrofloxacin composite nanogels in RAW 264.7 cells (n = 3). (A) Uptake of drugs at different time points. After removing the drugs: (B) phosphate-buffered saline; (C) Native enrofloxacin; (D) Enrofloxacin composite nanogels for 2 h, the confocal images of nanogels staying inside the cells, where the Hochest nuclear stain was shown in blue and fluorescein isothiocyanate isomer I-labeled nanogels were shown in green.

faster and more radical killing effects (**Fig. 5**). The bactericidal effect was observed when the concentrations of the enrofloxacin composite nanogels were all 2×MIC (4 µg/mL) at 48 h. When the concentration of enrofloxacin composite nanogels increases, it has significant bactericidal activity against SASCVs strain in a short time. Overall, the inhibitory effect increased with increasing drug concentration.

DISCUSSION

Recently, there has been increasing interest in combining the advantages of nanoparticles and hydrogels and preparing nanogels to enhance the bioadhesion capacity of an antibacterial drug to bacteria and cells, which in turn increases the intracellular therapeutic drug concentrations and the efficacy of the antibacterial drug against intracellular bacteria [22-24]. In this study, enrofloxacin-loaded gelatin-SA composite nanogels were formulated by electrostatic interactions between gelatin (positive charge) and SA (negative charge) with the help of $CaCl_2$ (ionic crosslinkers). The concentrations of SA, gelatin, and $CaCl_2$ were selected as variables to optimize the enrofloxacin composite nanogels by a single factor test using
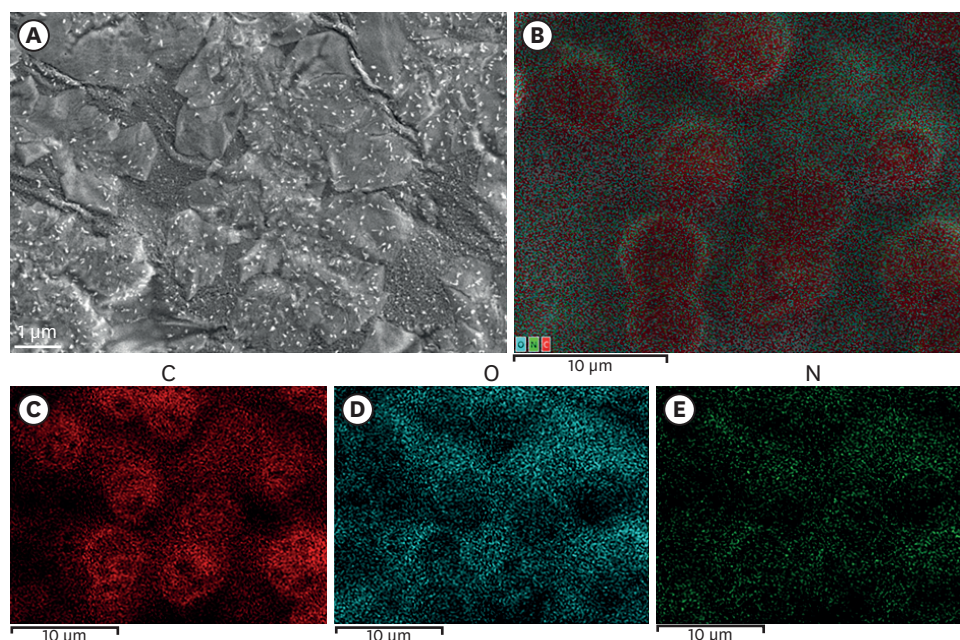
Fig. 4. Scanning electron microscopy images of co-culture of SASCVs strain and enrofloxacin composite nanogels for 30 min. (A) Enrofloxacin composite nanogels were contacted with or absorbed on the SASCVs strains; (B) Energy dispersive spectrometer images; (C) C element; (D) O element; (E) N element.
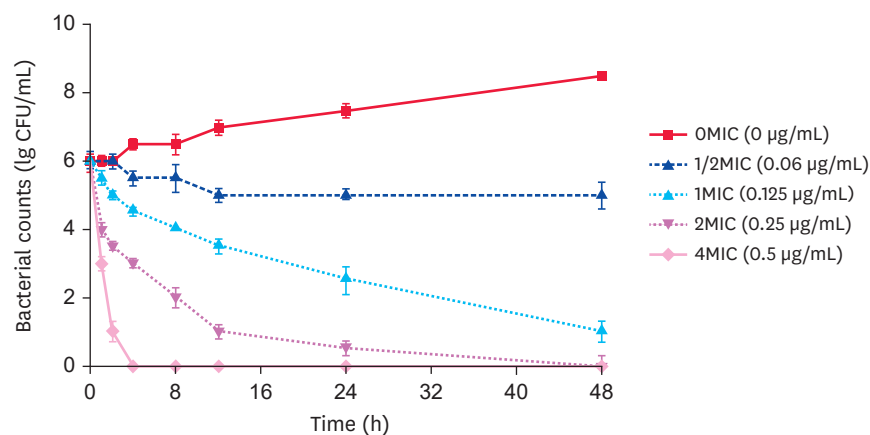SASCV, *Staphylococcus aureus* small colony variant.

Fig. 5. Killing rate curve of the enrofloxacin composite nanogels against the intracellular *Staphylococcus aureus* small colony variants.
MIC, minimum inhibitory concentration.

EE, LC, size, ZP, and PDI as the assessment indices. Smaller enrofloxacin composite nanogel particles could enter the host cells easily. By contrast, when the ZP of enrofloxacin composite nanogels was greater, it was easier to adsorb on the cell-membrane surface by electrostatic interactions. The dispersion of enrofloxacin composite nanogels was better when the PDI was smaller. Furthermore, the formation of enrofloxacin composite nanogels was more successful when the EE and LC of enrofloxacin composite nanogels were greater [11]. Hence, the optimal formula was comprised of 10 mg/mL (gelatin), 5 mg/mL (SA), and 0.25 mg/mL (CaCl$_2$). TEM showed that enrofloxacin composite nanogels were spherical with a smooth surface and good particle size distributions, implying that enrofloxacin composite nanogels had been formulated successfully by electrostatic interaction between the gelatin and SA

with the help of $CaCl_2$. On the other hand, the particle size of the enrofloxacin composite nanogels detected by TEM was smaller than that determined using the Zeta sizer ZX3600. The difference was because the particle size tested by the Zeta sizer ZX3600 was in the aqueous state, and so the sizes were the hydrated diameters. The particle size of enrofloxacin composite nanogels is usually larger than the real sizes. The particle sizes determined by TEM were smaller than genuine diameters because the free water and even some of the hydrated water had evaporated [9].

After the RAW 264.7 cells were incubated with 4 µg/mL native enrofloxacin and composite nanogels for 0.5, 1, 2, and 4 h, the drug uptake of enrofloxacin was increased significantly by the composite nanogels. This result shows that composite nanogels might increase the intracellular enrofloxacin delivery performance. Confocal microscopy also confirmed that many FITC-labeled enrofloxacin composite nanogels effectively entered the RAW 264.7 cells after co-incubation for 2 h. Interestingly, the labeled green fluorescence of enrofloxacin composite nanogels was stronger than the native enrofloxacin. Moreover, the enrofloxacin composite nanogels were internalized more easily into RAW 264.7 cells, which might be due to the cationic nature of gelatin interacting with the negative charge of the RAW 264.7 cells membrane and the adhesion of SA nanogels.

A co-culture of SASCVs strain and enrofloxacin composite nanogels for 30 min was observed by SEM to determine the bioadhesion capacity of enrofloxacin to bacteria. The enrofloxacin composite nanogels could enhance the bioadhesion capacity of enrofloxacin to the SASCVs because the cationic nature of gelatin in an acid medium interacts with the negative charge of the SASCVs strain and because of the excellent adhesion of SA. This might influence the integrity of the bacterial cell membranes or increase the drugs accessing bacteria, increasing the antibacterial activity of enrofloxacin [15]. The antimicrobial activity of the enrofloxacin composite nanogels against intracellular SASCVs strain was evaluated by MIC, MBC, MBIC, MBEC, and killing rate curve. The MIC, MBC, MBIC, and MBEC were 2, 4, 4, and 8 µg/mL, respectively. This suggests that enrofloxacin composite nanogels had strong antibacterial activity against the intracellular SASCVs. These results are consistent with the killing rate curve. When the concentration of the enrofloxacin composite nanogels increases, it has significant bactericidal activity against the intracellular SASCVs strain. Hence, the area under concentration–time curve/MIC might be the most suitable parameter to formulate the dosage regimen of the enrofloxacin composite nanogels against the intracellular SASCVs because of the concentration-dependent bactericidal effect [25]. Thus, the enrofloxacin composite nanogels might be a potential strategy to solve the therapy difficulty of SASCVs infections.

In conclusion, enrofloxacin-loaded gelatin-SA composite nanogels were formulated by electrostatic interactions between gelatin (positive charge) and SA (negative charge) using $CaCl_2$ (ionic crosslinkers) to enhance the efficacy of enrofloxacin against cow mastitis caused by SASCVs strain. The enrofloxacin-loaded gelatin-SA composite nanogels were homogenous canary yellow uniform suspension with a sedimentation rate of 1, spherical shape with a smooth surface, and particle size distributions of 323.2 ± 4.3 nm, PDI of 0.11 ± 0.02, ZP of −34.4 ± 0.8 mV, EE of 15.4% ± 0.2%, LC of 69.6% ± 1.3%, and sedimentation rate of 1. After the RAW 264.7 cells were incubated with enrofloxacin composite nanogels for 2 h, enrofloxacin composite nanogels were internalized more efficiently into cells. Interestingly, the enrofloxacin composite nanogels could enhance the bioadhesion capacity of enrofloxacin to the SASCVs by adhesive studies. Furthermore, MIC, MBC, MBIC, and MBEC were 2, 4, 4, and 8 µg/mL, respectively. The killing rate curve showed a concentration-dependent

bactericidal effect. Therefore, the prepared enrofloxacin composite nanogels might enhance the antibacterial activity of enrofloxacin against cow mastitis caused by SASCVs and other intracellular bacterial infections.

REFERENCES

1. Ogawa M, Takahashi M, Matsutani M, Takada N, Noda S, Saijo M. Obligate intracellular bacteria diversity in unfed *Leptotrombidium scutellare* larvae highlights novel bacterial endosymbionts of mites. Microbiol Immunol. 2020;64(1):1-9.
   PUBMED | **CROSSREF**

2. Svennesen L, Lund TB, Skarbye AP, Klaas IC, Nielsen SS. Expert evaluation of different infection types in dairy cow quarters naturally infected with *Staphylococcus aureus* or *Streptococcus agalactiae*. Prev Vet Med. 2019;167:16-23.
   PUBMED | **CROSSREF**

3. Ren Q, Liao G, Wu Z, Lv J, Chen W. Prevalence and characterization of *Staphylococcus aureus* isolates from subclinical bovine mastitis in southern Xinjiang, China. J Dairy Sci. 2020;103(4):3368-3380.
   PUBMED | **CROSSREF**

4. Mphahlele MP, Oguttu JW, Petzer IM, Qekwana DN. Prevalence and antimicrobial drug resistance of *Staphylococcus aureus* isolated from cow milk samples. Vet World. 2020;13(12):2736-2742.
   PUBMED | **CROSSREF**

5. Alkasir R, Liu X, Zahra M, Ferreri M, Su J, Han B. Characteristics of *Staphylococcus aureus* small colony variant and its parent strain isolated from chronic mastitis at a dairy farm in Beijing, China. Microb Drug Resist. 2013;19(2):138-145.
   PUBMED | **CROSSREF**

6. Watanabe Y, Oikawa N, Hariu M, Seki M. Evaluation of agar culture plates to efficiently identify small colony variants of methicillin-resistant *Staphylococcus aureus*. Infect Drug Resist. 2019;12:1743-1748.
   PUBMED | **CROSSREF**

7. Meng K, Chen D, Yang F, Zhang A, Tao Y, Qu W, et al. Intracellular delivery, accumulation, and discrepancy in antibacterial activity of four enrofloxacin-loaded fatty acid solid lipid nanoparticles. Colloids Surf B Biointerfaces. 2020;194:111196.
   PUBMED | **CROSSREF**

8. Luo W, Chen D, Wu M, Li Z, Tao Y, Liu Q, et al. Pharmacokinetics/Pharmacodynamics models of veterinary antimicrobial agents. J Vet Sci. 2019;20(5):e40.
   PUBMED | **CROSSREF**

9. Liu Y, Chen D, Zhang A, Xiao M, Li Z, Luo W, et al. Composite inclusion complexes containing hyaluronic acid/chitosan nanosystems for dual responsive enrofloxacin release. Carbohydr Polym. 2021;252:117162.
   PUBMED | **CROSSREF**

10. Ahmed S, Alhareth K, Mignet N. Advancement in nanogel formulations provides controlled drug release. Int J Pharm. 2020;584:119435.
    PUBMED | **CROSSREF**

11. Algharib SA, Dawood A, Zhou K, Chen D, Li C, Meng K, et al. Designing, structural determination and biological effects of rifaximin loaded chitosan-carboxymethyl chitosan nanogel. Carbohydr Polym. 2020;248:116782.
    PUBMED | **CROSSREF**

12. Wei X, Xiong H, Zhou D, Jing X, Huang Y. Ion-assisted fabrication of neutral protein crosslinked sodium alginate nanogels. Carbohydr Polym. 2018;186:45-53.
    PUBMED | **CROSSREF**

13. Zhou K, Wang X, Chen D, Yuan Y, Wang S, Li C, et al. Enhanced treatment effects of tilmicosin against *Staphylococcus aureus* cow mastitis by self-assembly sodium alginate-chitosan nanogel. Pharmaceutics. 2019;11(10):524.
    PUBMED | **CROSSREF**

14. Wu D, Wan M. A novel ultrasonic-triggered drug release and tracked drug delivery system based on gas-filled BSA microbubbles and gelatin nanogels. J Control Release. 2015;213:e24.
    PUBMED | **CROSSREF**

15. Madhusudana Rao K, Krishna Rao KS, Ramanjaneyulu G, Ha CS. Curcumin encapsulated pH sensitive gelatin based interpenetrating polymeric network nanogels for anti cancer drug delivery. Int J Pharm. 2015;478(2):788-795.
    PUBMED | **CROSSREF**

16. Luo J, Gao Y, Liu Y, Huang X, Zhang DX, Cao H, et al. Self-assembled degradable nanogels provide foliar affinity and pinning for pesticide delivery by flexibility and adhesiveness adjustment. ACS Nano. 2021;15(9):14598-14609.
PUBMED | CROSSREF

17. Liu Y, Cui X, Zhao L, Zhang W, Zhu S, Ma J. Chitosan nanoparticles to enhance the inhibitory effect of natamycin on *Candida albicans*. J Nanomater. 2021;2021:6644567.
CROSSREF

18. Zhang W, Bao B, Jiang F, Zhang Y, Zhou R, Lu Y, et al. Promoting oral mucosal wound healing with a hydrogel adhesive based on a phototriggered S-nitrosylation coupling reaction. Adv Mater. 2021;33(48):e2105667.
PUBMED | CROSSREF

19. Suo H, Hussain M, Wang H, Zhou N, Tao J, Jiang H, et al. Injectable and pH-sensitive hyaluronic acid-based hydrogels with on-demand release of antimicrobial peptides for infected wound healing. Biomacromolecules. 2021;22(7):3049-3059.
PUBMED | CROSSREF

20. Campana R, Casettari L, Fagioli L, Cespi M, Bonacucina G, Baffone W. Activity of essential oil-based microemulsions against *Staphylococcus aureus* biofilms developed on stainless steel surface in different culture media and growth conditions. Int J Food Microbiol. 2017;241:132-140.
PUBMED | CROSSREF

21. Shu M, Long S, Huang Y, Li D, Li H, Li X. High strength and antibacterial polyelectrolyte complex CS/HS hydrogel films for wound healing. Soft Matter. 2019;15(38):7686-7694.
PUBMED | CROSSREF

22. Peng H, Huang X, Melle A, Karperien M, Pich A. Redox-responsive degradable prodrug nanogels for intracellular drug delivery by crosslinking of amine-functionalized poly(N-vinylpyrrolidone) copolymers. J Colloid Interface Sci. 2019;540:612-622.
PUBMED | CROSSREF

23. Algharib SA, Dawood A, Xie S. Nanoparticles for treatment of bovine *Staphylococcus aureus* mastitis. Drug Deliv. 2020;27(1):292-308.
PUBMED | CROSSREF

24. Zhou K, Li C, Chen D, Pan Y, Tao Y, Qu W, et al. A review on nanosystems as an effective approach against infections of *Staphylococcus aureus*. Int J Nanomedicine. 2018;13:7333-7347.
PUBMED | CROSSREF

25. Luo W, Qin H, Chen D, Wu M, Meng K, Zhang A, et al. The dose regimen formulation of tilmicosin against *Lawsonia intracellularis* in pigs by pharmacokinetic-pharmacodynamic (PK-PD) model. Microb Pathog. 2020;147:104389.
PUBMED | CROSSREF